# Computational Study of Matrix−Peptide Interactions in MALDI Mass Spectrometry: Interactions of 2,5- and 3,5-Dihydroxybenzoic Acid with the Tripeptide Valine−Proline−Leucine

**Faten H. Yassin and Dennis S. Marynick***

*Department of Chemistry and Biochemistry, University of Texas at Arlington, Arlington, Texas 76019-0065*

*Received: September 21, 2005*

The mechanism of matrix-to-analyte proton transfer in matrix-assisted laser desorption and ionization mass spectrometry (MALDI-MS) has been investigated computationally by modeling the matrix−analyte interaction of potential MALDI matrixes such as 2,5-dihydroxybenzoic acid (2,5-DHB) and 3,5-DHB with the tripeptide valine−proline−leucine (VPL). A combination of molecular dynamics/simulated annealing calculations followed by density functional theory geometry optimization using a reasonably large basis set has been done on a large number of clusters in an attempt to study the ionization energy of each matrix in the cluster environment and the intracluster proton transfer from the matrix to the tripeptide. The calculations show a substantial reduction in the IP for both matrixes in their cluster environments. In the 2,5-system, proton transfer can sometimes occur in the neutral clusters (preformed ions), whereas proton transfer in the cationic clusters, which is actually a double proton transfer, is spontaneous and exoergic. Even though it is more acidic from a thermodynamic perspective, the radical cation of 3,5-DHB is a less efficient proton donor to VPL. The thermodynamics of proton transfer in the cationic clusters is discussed in detail.

## Introduction

Understanding the mechanism of ionization processes involved in matrix-assisted laser desorption and ionization mass spectrometry (MALDI-MS) is still a challenging area of research. These processes are generally divided into two categories: primary and secondary ionization. The primary ionization processes occur during or shortly after the laser pulse and include the formation pathways of the first (primary) ions from the neutral species in the matrix/peptide sample (here we restrict our study to MALDI spectrometry on proteins). These ions are often matrix-derived species. Secondary ions are generated in the ensuing desorption plume and result in the formation of analyte ions. In the mass spectrum, primary and secondary ions are both usually observed. Secondary reactions have been found to be largely under thermodynamic control. In other words, if the relevant gas-phase thermodynamic data are available, secondary processes would be relatively straightforward to predict.[1,2]

Our research focuses on developing fundamental understanding of the matrix-to-analyte proton transfer in MALDI. Several mechanistic studies have been published in attempts to understand the proton-transfer reactions from matrix-derived species to the analyte.[3] Zenobi and Knochenmuss have published an excellent review of these studies.[2] Our interest in this subject has resulted in several experimental and theoretical studies,[4−9] in attempts to clarify the main aspects of matrix-to-analyte proton transfer. Here, we will briefly summarize these studies and rationalize our foundations.

To effectively approach this mechanistic problem, it has been essential to study (1) relevant thermodynamic properties of MALDI species and (2) the nature of the specific matrix/analyte interactions leading to proton transfer. One of our ongoing research areas is investigating thermodynamic properties such as the ionization potential (IP), gas-phase acidity (GA), gas-phase basicity (GB), and gas-phase proton affinity (PA) of potential MALDI matrixes.[6−9] We found that thermodynamic properties such as GB, gas-phase PA, and GA of the neutral and radical cation form of the matrix are not always predictive of efficient MALDI matrixes; however, the IP of the matrix may play a more important role. Earlier studies have shown that most MALDI matrixes have IPs that lie above the two photon threshold of the nitrogen laser. These studies suggest the possibility of specific matrix−analyte interactions that result in substantial reductions in the IPs of the matrix/analyte clusters as compared to the IPs of the free MALDI matrixes.[2,10−17] In this area, we have previously studied both computationally and experimentally the essential interactions in small clusters of the common MALDI matrix 2,5-dihydroxybenzoic acid (2,5-DHB) with the amino acids proline and arginine.[4,5] We found that hydrogen-bonding interactions between the matrix and the analyte have a large effect on the electronic structure of the matrix, lowering the IP of 2,5-DHB well below 7.5 eV, the two photon threshold of the nitrogen laser. In efforts to approach better MALDI realistic models, Kinsel et al. have also experimentally studied the mechanism of matrix-to-analyte proton transfer in neutral clusters of 2,5-DHB and the tripeptide valine−proline−leucine (VPL).[18] These studies showed a reduction in the IP of 2,5-DHB$_m$/VPL$_n$ clusters of greater than 1 eV as comparing to the IP (8.05 eV) of free 2,5-DHB for large clusters ($m$ or $n$ greater than 1). In addition, proton transfer is initiated by formation of the cluster radical cation. It was also found that the IP of the 2,5-DHB/VPL ($m = n = 1$) cluster is between 6.99 and 8.05 eV.

In this paper, we extend the previous work on the 2,5-DHB/VPL system by presenting an extensive computational study

* To whom correspondence should be addressed. E-mail: dennis@uta.edu.

10.1021/jp058257c CCC: $33.50 
Published on Web 02/09/2006

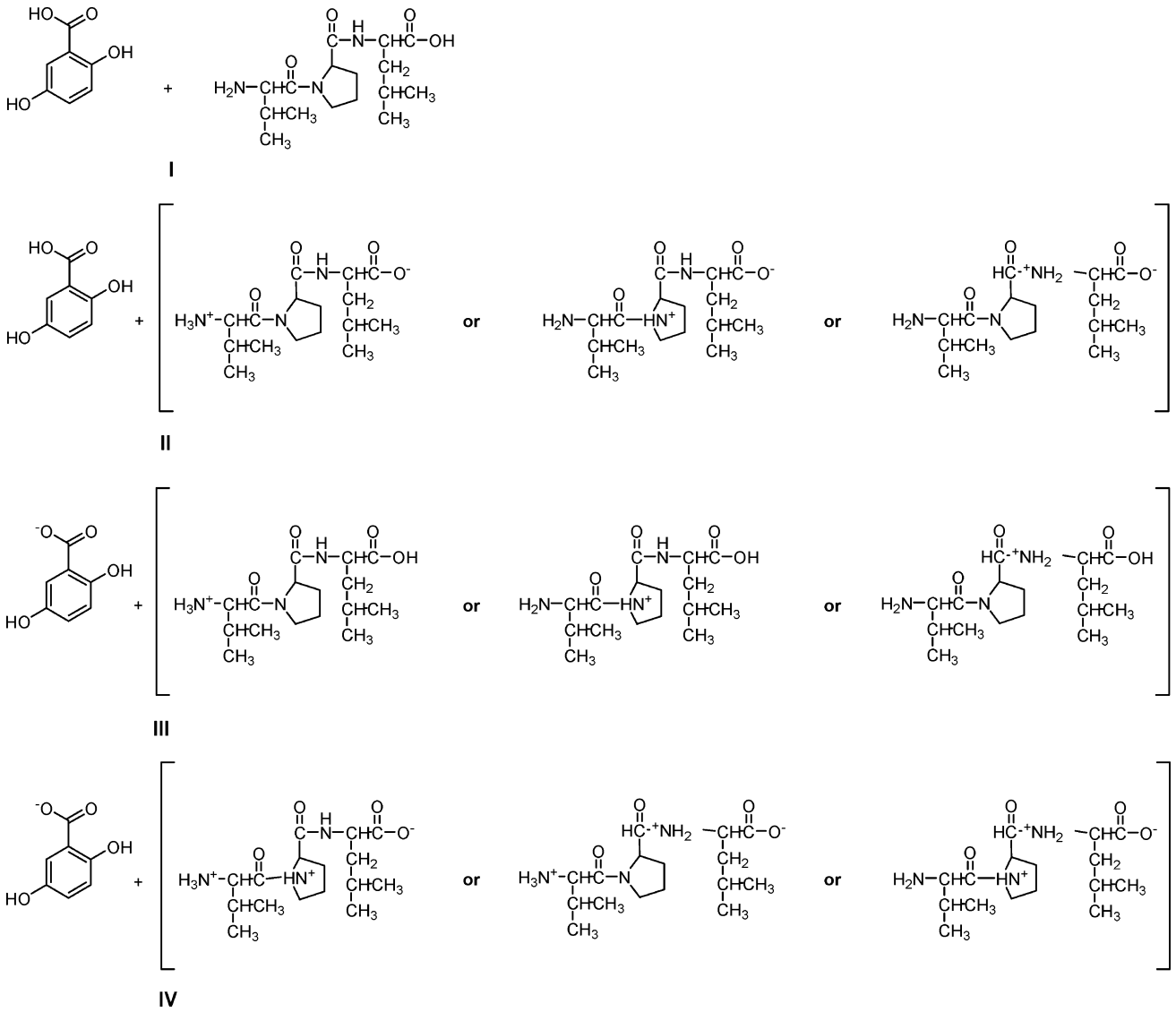


**Figure 1.** Starting points for molecular dynamics simulations. (I) DHB + canonical VPL, (II) DHB + zwitterionic VPL, (III) deprotonated DHB + canonical-protonated VPL, and (IV) deprotonated DHB + zwitterionic-protonated VPL.

of the same system. In addition, to probe the differences between an active MALDI matrix and a similar but totally inactive one, we present a parallel study of the 3,5-DHB/VPL system. One aim of this computational study is to provide insights into the mechanism of the IP reduction and matrix-to-analyte proton transfer that occur in neutral and cationic 2,5-DHB/VPL clusters. Another aim is to demonstrate important features that make 2,5-DHB an efficient matrix and 3,5-DHB a nonfunctional matrix. The structures and intermolecular interactions involved that lead to IP reduction of these matrixes are characterized and reported in this paper for both clusters. Finally, we investigate the analyte protonation, which is a key aspect of secondary ionization reactions, in the two clusters. Donation of a proton from the matrix to analyte is found to proceed without barrier in many of the cationic complexes, and in some of the neutral systems. In addition, the key structural and electronic differences between 2,5-DHB and 3,5-DHB leading to the former being a superior matrix, are discussed.

## Computational Methodology

Molecular dynamics and simulated annealing were performed to identify the candidate structures for each of the two clusters (VPL/2,5-DHB and VPL/3,5-DHB) starting from (1) DHB + canonical VPL, (II) DHB + zwitterionic VPL, (III) deprotonated DHB + canonical-protonated VPL, (IV) deprotonated DHB + zwitterionic-protonated VPL (Figure 1). All possible sites of protonation were considered, resulting in 10 chemically distinct clusters for each matrix. Deprotonation of the matrix in the neutral clusters was assumed to occur at the carboxylic acid site, because our previous studies have shown that this is the most acidic site for both DHB isomers.[7] The MMFF force field was used to find the candidate structures for each system. During the molecular dynamic (MD) simulations, the systems were heated to 1200 K in 40 ps followed by a run time of 60 ps and cooled to 20 K in 40 ps. The candidate structures were then optimized at the HF/3-21G level. All structures within 50 kJ/mol of the lowest-energy structure at this level were then optimized using the B3LYP[19] functional with the 6-31+G** basis set on the O, N, and H atoms and the 6-31G** basis set on the carbon atoms (B3LYP/gen). All structures were characterized as true minima on the potential energy surfaces by vibrational frequency analysis at the same level of theory. The final electronic energies of all the structures within 25 kJ/mol of the lowest energy structure at the B3LYP/gen level were then determined at the B3LYP/6-311++G (2df, 2p)//B3LYP/gen level. Vertical IPs were calculated as the energy difference

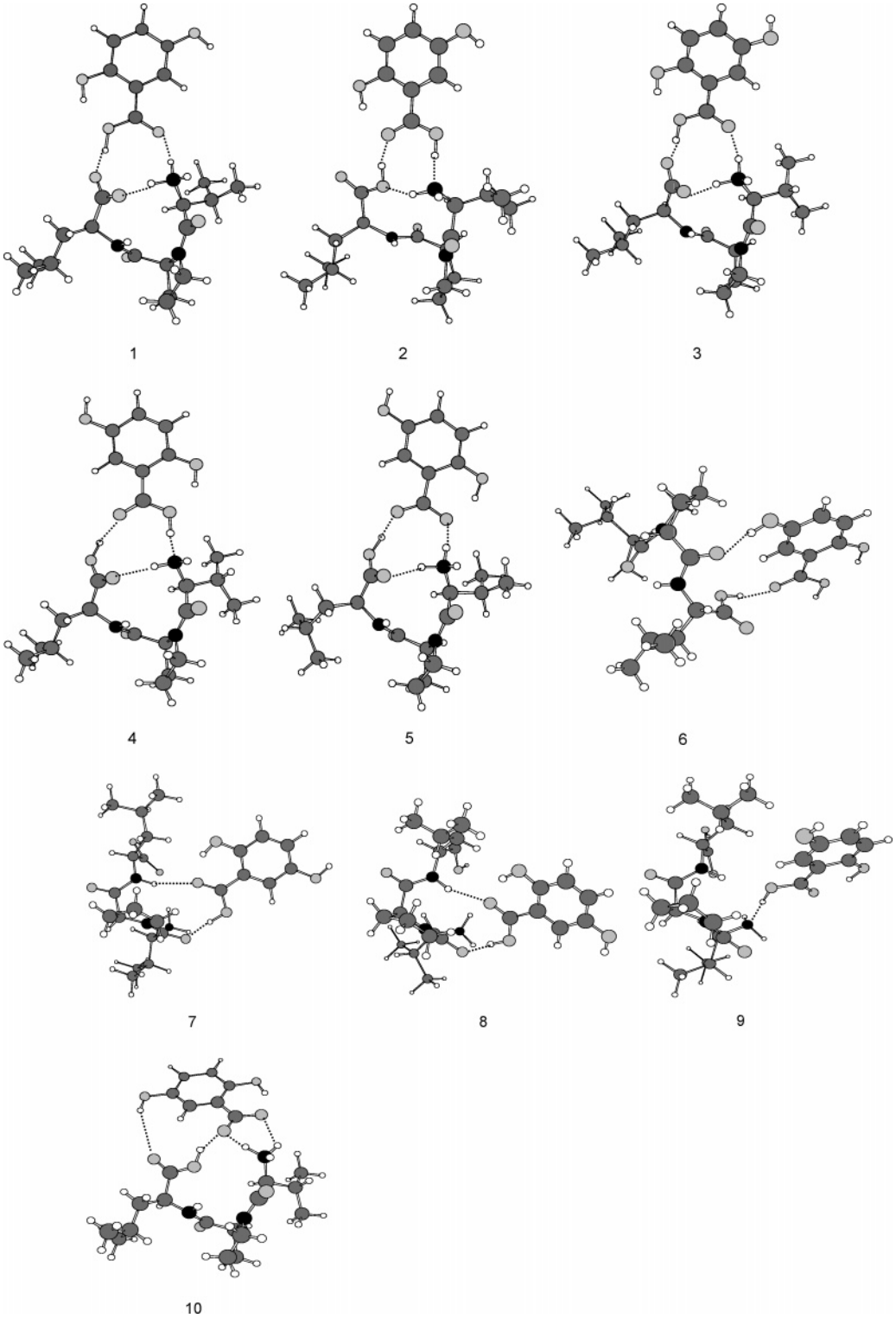


**Figure 2.** Ten minima for the 2,5-DHB/VPL gas-phase complex at the B3LYP/gen level.

between the neutral and ionized species at the geometry of the neutral species. This level of theory has been shown to yield accurate IP's for five related systems: 2,5-DHB, 2,3-DHB, 2,5-DHB(proline)$_1$, 2,5-DHB(proline)$_2$ and 2,5-DHB−(proline)$_4$. The average absolute error is only 0.10 eV, but the error is highly systematic, with the calculated values being too high. Koopmans' theorems IPs (KTIPs) were calculated at the HF/gen//B3LYP/gen level. Group natural charges[20] and Mulliken spin populations were determined at the B3LYP/gen level.

The MD simulations were carried out using macromodel 8.1 from Schrodinger, Inc.[21] Ab initio and DFT calculations were carried out using the Gaussian 03[22] suite of programs.

## Results and Discussion

**2,5-DHB/VPL Clusters.** Ten distinct minima (Figure 2) within 21.2 kJ/mol of each other were found at the B3LYP/gen level (Table 1).

**TABLE 1: Calculated Relative Energies and Ionization Potentials of the 2,5-DHB/VPL Clusters[a,b]**

| | B3LYP/Gen | | | | B3LYP/6-311++G(2df,2p)//B3LYP/Gen | | HF/Gen |
|---|---|---|---|---|---|---|---|
| cluster | relative energy (kJ/mol) | IP (eV)[c] | group charge | spin population | relative energy (kJ/mol) | IP (eV) | KTIP[d] (eV) |
| 1 | 0.0 | 7.49 | −0.10 | 0.76 | 0.0 | 7.62 | 8.10 |
| 2 | 2.0 | 7.56 | −0.10 | 0.73 | 0.6 | 7.67 | 8.21 |
| 3 | 1.8 | 7.45 | −0.10 | 0.76 | 1.6 | 7.56 | 8.05 |
| 4 | 9.9 | 7.52 | −0.10 | 0.72 | 8.0 | 7.63 | 8.17 |
| 5 | 8.6 | 7.17 | −0.21 | 0.91 | 9.1 | 7.28 | 7.67 |
| 6 | 20.5 | 7.49 | 0.00 | 0.75 | 12.3 | 7.60 | 8.12 |
| 7 | 20.4 | 7.49 | −0.05 | 0.66 | 12.5 | 7.61 | 8.26 |
| 8 | 20.8 | 7.69 | −0.05 | 0.70 | 13.4 | 7.80 | 8.39 |
| 9 | 21.3 | 7.47 | −0.11 | 0.74 | 17.9 | 7.58 | 8.13 |
| 10 | 19.4 | 7.10 | −0.28 | 0.97 | 21.2 | 7.20 | 7.59 |

[a] All energies were evaluated at the B3LYP/gen optimized geometries. [b] IP is in eV, $\Delta E$ in kJ/mol. [c] The calculated IP of free 2,5-DHB at this level is 8.06 eV. [d] The calculated KTIP of free 2,5-DHB at this level is 8.39 eV. Geometries optimized at the B3LYP/gen level.

**TABLE 2: Calculated Relative Energies and Ionization Potentials of the 3,5-DHB/VPL Clusters[a,b]**

| | B3LYP/Gen | | | | B3LYP/6-311++G(2df, 2p)//B3LYP/Gen | | HF/Gen |
|---|---|---|---|---|---|---|---|
| cluster | relative energy (kJ/mol) | IP (eV)[c] | group charge | spin population | relative energy (kJ/mol) | IP (eV) | KTIP (eV)[d] |
| 1 | 0.0 | 7.70 | −0.09 | 0.76 | 0.0 | 7.80 | 8.36 |
| 2 | 11.5 | 7.73 | 0.00 | 0.46 | 4.6 | 7.84 | 8.82 |
| 3 | 12.7 | 7.79 | −0.06 | 0.57 | 13.6 | 7.89 | 8.70 |
| 4 | 19.4 | 7.78 | −0.08 | 0.54 | 17.1 | 7.88 | 8.76 |
| 5 | 18.7 | 7.65 | −0.09 | 0.80 | 17.4 | 7.76 | 8.32 |
| 6 | 21.1 | 7.77 | −0.06 | 0.82 | 28.2 | 7.85 | 8.44 |

[a] All energies were evaluated at the B3LYP/gen optimized geometries. [b] IP is in eV, $\Delta E$ in kJ/mol [c] The calculated IP of free 3,5-DHB at this level is 8.47 eV. [d] The calculated KTIP of free 3,5-DHB at this level is 8.82 eV.

Six of these structures are of type I (2,5-DHB + canonical VPL), two of them are of type II (2,5-DHB + zwitterionic VPL), and two are of type IV (deprotonated 2,5-DHB + zwitterionic protonated VPL). No structures are of type III (deprotonated 2,5-DHB + canonical protonated VPL). Although the majority of these conformers are of type I, the lowest-energy structure is of type II.

To investigate the effects of the matrix-to-analyte interactions on the electronic structure, the change in the IP of free 2,5-DHB compared to that for 2,5-DHB in each of the cluster environments has been calculated at the B3LYP/gen and B3LYP/6-311++G (2df, 2p)//B3LYP/gen levels (see Figure 2 and Table 1). The IP of free 2,5-DHB at the former level is 8.06 eV. The IPs decrease an average of about 0.6 eV in each of these clusters except for clusters 5 and 10. These clusters exhibit a ground-state matrix-to-analyte proton transfer and have very low IPs (7.28 and 7.20 eV, respectively) because the DHB moiety is formally an anion. The vertical IP of the lowest energy structure is 7.62 eV, well within the rather broad experimental range of 6.99−8.05 eV.[18]

The KTIP of free 2,5-DHB is 8.39 eV. On going from the free 2,5-DHB to 2,5-DHB in each of the clusters excluding clusters 5 and 10, the KTIP drops on average about 0.2 eV, or about half of the average vertical IP reduction of 0.6 eV. Because KTIPs only take ground states into account, it is clear that only part of the overall IP reduction is a ground-state effect. As we demonstrated[4] in our earlier work on the proline/2,5-DHB system, the ground state effect is associated with a build up of charge on the 2,5-DHB via inductive donation (principally hydrogen bonding between DHB OH groups and the nitrogens in the peptide). This results in a net negative group charge on the 2,5-DHB, which raises the energy of all of the frontier orbitals and lowers the IP. This is clearly indicated by natural population analysis, which yield an average group charge of $-0.10e^-$ on 2,5-DHB (Table 1). The second important mechanism for the lowering of the IP is spin delocalization in the ion state. In the radical cation, an electron has been ionized from the $\pi$ system of the 2,5-DHB, leaving one unpaired electron on 2,5-DHB. This unpaired electron is partially delocalized over both molecules. Mulliken population analyses (Table 1) confirm that the unpaired electron is distributed on average about 70% on the 2,5-DHB and 30% on the VPL. This electron delocalization stabilizes the cation in the ionized structure and lowers the IP.

**3,5-DHB/VPL Clusters.** Six distinct minima (Figure 3) within 28.2 kJ/mol of each other were found at the B3LYP/gen level (Table 2). Four of these structures are of type I, including the lowest energy conformer. The third and sixth conformers are of type II. The calculated IPs vary from 7.76 to 7.89 eV. There are no experimental data available in the literature for this system.

A distinct and possibly very important difference between the 2,5- and 3,5-DHB clusters is that there are no energetically competitive 3,5-DHB clusters in which the proton has transferred in the ground (neutral) state. The lowest energy structure of this type (not shown) is about 50 kJ/mol less stable than the minimum energy cluster reported in Table 2. In comparison, the most stable 2,5-DHB/VPL cluster exhibiting proton transfer in the ground state is only 9 kJ/mol less stable than the minimum energy cluster (cluster 5, Table 1). This is fully consistent with the relative gas-phase acidities of neutral 2,5-DHB (1331 kJ/mol) and 3,5-DHB (1374 kJ/mol).

The IP of free 3,5-DHB is 8.47 eV at the B3LYP/gen level, which is significantly higher than any of the IPs of all of the reported clusters. Similar effects are seen in these clusters. Both ground and ion state effects are operative; however, the cluster IPs are in general somewhat higher than those found in the 2,5-DHB system. This is not surprising given that the IP of free 3,5-DHB is about 0.4 eV higher than that of the 2,5-isomer.

**Proton Transfer in the Cationic Clusters.** In attempts to investigate the structural rearrangement occurring in the cationic clusters immediately following ionization, the geometries of all

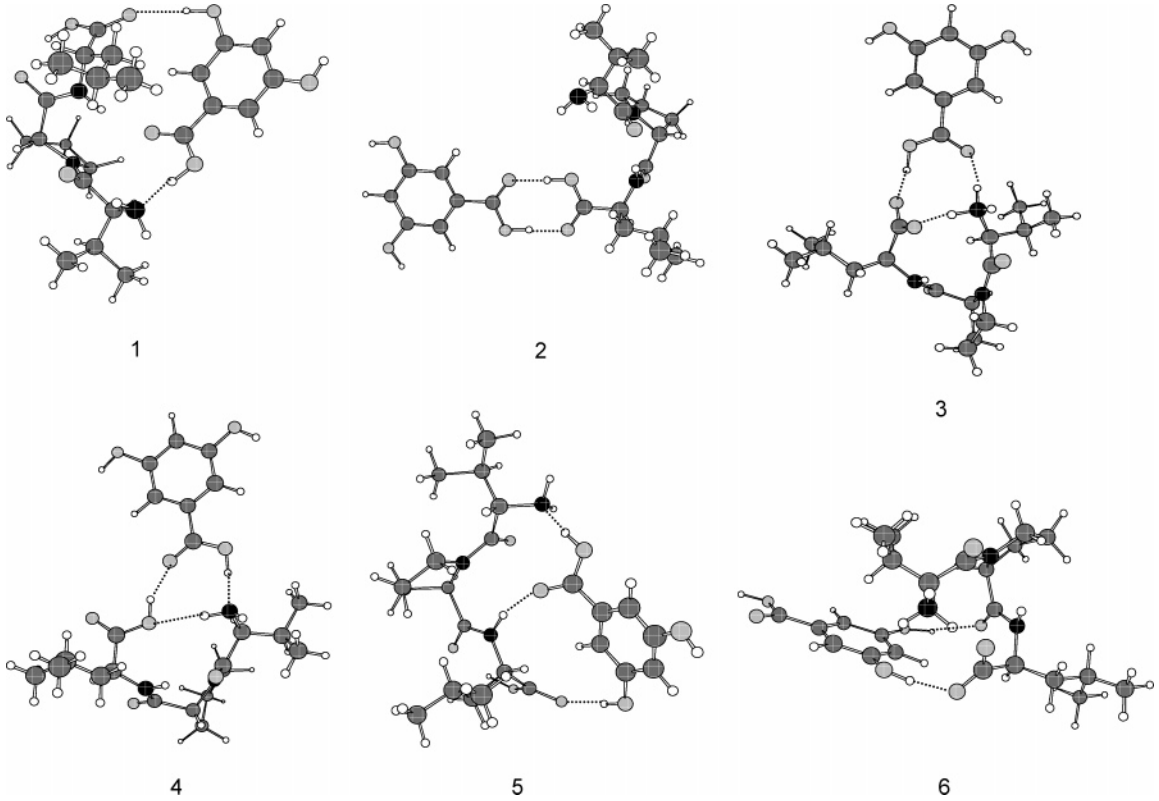


**Figure 3.** Six minima for the 3,5-DHB/VPL gas-phase complex at the B3LYP/gen level.

the ionized species were allowed to relax at the B3LYP/gen level. In most 2,5-DHB and 3,5-DHB cationic clusters, a proton transfer from the matrix to the tripeptide occurs via an exoergic reaction without a barrier.[23] In the 2,5-DHB clusters, proton transfer does not occur in clusters 5, 6 and 10 (for clusters 5 and 10, the proton transfer occurs before ionization). For the 3,5-DHB system, no proton transfer is observed in clusters 2 and 3. In all but one case (cluster 4 of the 3,5-DHB/VLP system), the carboxylic acid proton transfers to VPL; however, in the 2,5-DHB system, there is a second intramolecular proton transfer from the 2-OH group to the carboxylic acid group. If **A** is the proton accepting group, then the proton-transfer step occurs as follows:

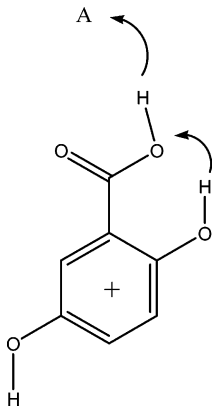


Two of these relaxed structures, corresponding to clusters 2 and 3 of the 2,5-DHB system, are shown in Figure 4. The double proton transfer is apparent in both. The overall matrix → peptide proton transfer reaction is much more exoergic for the 2,5-DHB clusters than for those of 3,5-DHB, especially for the lowest energy clusters (Table 3). At first, this might seem surprising, because the gas-phase acidity of free 2,5-DHB$^{\bullet+}$ is approximately 18 kJ/mol greater than that of 3,5-DHB$^{\bullet+}$, thus 3,5-DHB$^{\bullet+}$ is *more* acidic than 2,5-DHB$^{\bullet+}$. (Recall that the gas-phase acidity is defined as the free energy change for the

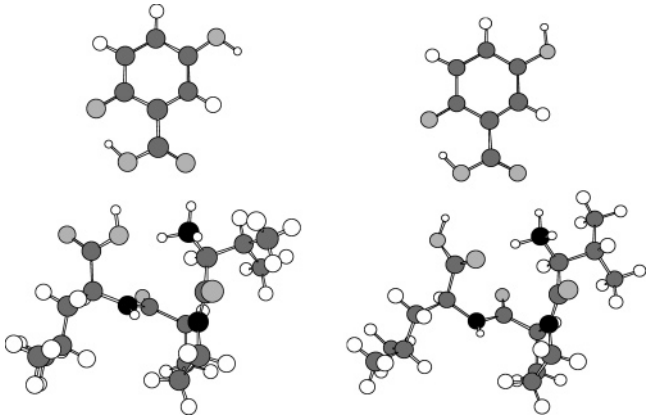

**Figure 4.** Optimized structures for the cations of clusters 2 and 3 for the 2,5-DHB/VPL system showing the double proton transfer.

**TABLE 3: Energetics of Proton Transfer for the Cationic Clusters**[a]

| | matrix | |
|---|---|---|
| cluster | 2,5-DHB | 3,5-DHB |
| 1 | −95.7 | −49.2 |
| 2 | −83.4 | no proton transfer |
| 3 | −97.0 | no proton transfer |
| 4 | −110.2 | −25.3 |
| 5 | *b* | −50.7 |
| 6 | no proton transfer | −96.5 |
| 7 | −27.0 | |
| 8 | −43.7 | |
| 9 | −102.1 | |
| 10 | *b* | |

[a] kJ/mol, at the B3LYP/gen//B3LYP/gen level. [b] Proton transfers in neutral clusters

deprotonation reaction; therefore the larger the gas-phase acidity, the weaker the acid.) Free 2,3-DHB is more acidic than the 2,5 isomer because the site of deprotonation is the 2-OH group in the former, which is subsequently stabilized by hydrogen bonding interactions from both the COOH and 3-OH group. This double hydrogen bond stabilization cannot be achieved in 2,5-DHB because the site of deprotonation is the 5-OH group. However, the relevant comparison for these clusters is not the overall gas-phase acidity, but rather the acidity *of the protons actually involved in the proton transfer, in this case the carboxylic acid* protons. Although the most acidic protons in both radical cations are on the OH groups, the carboxylic acid proton of 2,5-DHB$^{\bullet+}$ is far more acidic than that of the 3,5-isomer.[24] This is almost entirely due to the stabilizing effect of the ortho OH group and is likely to be a key difference between the two matrixes. Indeed, many (but not all) effective MALDI matrixes share this same structural feature: the *ortho* juxtaposition of a carboxylic acid group and a phenol group.

## Conclusion

Based on our current results and others, it seems clear that the efficiency of a MALDI matrix is strongly controlled by a number of factors. Certainly the IP of the matrix, or more specifically the IP of the matrix bound to the analyte, is important. Matrix−analyte interactions play a major role in lowering the IP of the matrix. However, this lowering may not be sufficient enough to reduce the IP of a potential MALDI matrix to below the two-photon threshold of the nitrogen laser if the IP of the pure matrix is too high.

Our results also suggest that preformed ions, resulting from a proton transfer from the carboxylic acid group to the peptide, may also play an important role in the MALDI process. We observed two low-energy structures of this type for the 2,5-DHB/VPL clusters, whereas there are no such energetically accessible structures for the 3,5-DHB/VPL system. This is consistent with the relative gas-phase acidities of the neutral matrixes and is potentially important because the IPs of these ion-pair clusters are quite low (7.2−7.3 eV) and are well-below the two photon threshold of the nitrogen laser (7.5 eV).

We also have shown that proton transfer in the cationic species for the 2,5-DHB/VPL system is a spontaneous, barrierless and exoergic process that occurs via a double proton transfer: The carboxylic acid proton undergoes an intermolecular transfer to the peptide whereas the 2-OH proton on DHB undergoes an intramolecular transfer to the carboxylic acid group. This led to the important conclusion that, when the thermodynamics of proton transfer are considered, the usual thermodynamic information, which is based on the lowest energy structure or, more correctly, a Boltzmann average of the thermally accessible structures, is insufficient. Rather, one must know the thermodynamic properties associated with the specific proton involved in the donation.

Are these results relevant to a real MALDI experiment on a protein? One clear limitation is the use of a tripeptide to model a protein. All of our calculated structures for both systems exhibit matrix hydrogen bonding to either the C or the N terminus of VPL. Because a typical MALDI analyte is usually a long polypeptide or a whole protein, our results may overemphasize the involvement of the termini. Nevertheless, we think it is likely that many of the fundamental ideas explored here will carry over to more realistic models. Indeed, current work on more realistic models, where the tripeptides are capped to eliminate hydrogen bonding and a wider variety of tripeptides and matrixes are examined, will verify the importance of preformed ions, IP reductions and matrix radical cation acidities.[25]

**Acknowledgment.** We acknowledge financial support from the Welch Foundation (Y-0743). We also thank Professor Gary Kinsel for helpful discussion and Dr. Kaori Ueno-Noto for assistance with some of the calculations.

**Supporting Information Available:** Optimized Cartesian coordinates for each cluster are available free of charge via the Internet at http://pubs.acs.org.

## References and Notes

(1) Zenobi, R.; Knochenmuss, *R. Mass Spectrom. Rev.* **1998**, *7*, 337.
(2) Knochenmuss, R.; Stortelder, A.; Breuker, K.; Zenobi, R. *J. Mass Spectrom.* **2000**, *35*, 1237.
(3) Liao, P.-C.; Allison, J. *J. Mass Spectrom.* **1995**, *30*, 408.
(4) Kinsel, G. R.; Knochenmuss, R.; Setz, P.; Land, C. M.; Goh, S.-K.; Archibong, E. F.; Hardesty, J. H.; Marynick, D. S. *J. Mass Spectrom.* **2002**, *37*, 1131.
(5) Kinsel, G. R.; Zhao, Q.; Narayanasamy, J.; Yassin, F. H.; Dias, H. V. R.; Niesner, B.; Prater, K.; Marie, C. St., Ly, L.; Marynick, D. S. *J. Phys. Chem. A* **2004**, *108*, 3153.
(6) Yassin, F. H.; Marynick, D. S. *J. Mol. Struct. THEOCHEM* **2003**, *629*, 223.
(7) Yassin, F. H.; Marynick, D. S. *Mol. Phys.* **2005**, *103*, 183.
(8) Yassin, F. H.; Marynick, D. S. Manuscript in preparation.
(9) Kinsel, G. R.; Yassin, F. H.; Marynick, D. S. Manuscript in preparation.
(10) Huang Y.; Russell, D. H. *Int. J. Mass Spectrom. Ion Processes* **1998**, *175*, 187.
(11) Land C. M.; Kinsel, G. R. *J. Am. Aoc. Mass Spectrom.* **1998**, *9*, 1060.
(12) Land C. M.; Kinsel, G. R. *Eur. Mass Spectrom.* **1999**, *5*, 117.
(13) Land C. M.; Kinsel, G. R. *J. Am. Soc. Mass Spectrom.* **2001**, *12*, 726.
(14) Krutchinsky, A. N.; Dolguine, A. I.; Khodorkovski, M. A. *Anal. Chem.* **1995**, *67*, 1963.
(15) Meffert A.; Grotemeyer, J. *Ber. Bunsen-Ges.*. **1998**, *102*, 459.
(16) Meffert A.; Grotemeyer, J. *Eur. Mass Spectrom.* **1995**, *1*, 594.
(17) Meffert A.; Grotemeyer, J. *Int. J. Mass Spectrom.* **2001**, *210/211*, 521.
(18) Land, C. M.; Kinsel, G. R. *J. Am. Soc. Mass Spectrom*. **2001**, *12*, 726.
(19) (a) Becke, A. D. *J. Chem. Phys.* **1993**, *98*, 5648. (b) Lee, C.; Yang, W.; Parr, R. G. *Phys. Rev. B* **1988**, *37*, 785.
(20) Reed, A. E.; Curtiss, L. A.; Weinhold, F. *Chem. Rev.* **1988**, *88*, 899.
(21) Mohamadi, F.; Richards, N. G. J.; Guida, W. C.; Liskamp, R.; Lipton, M.; Caufield, C.; Chang, G.; Hendrickson, T.; Still, W. C. *J. Comput. Chem.* **1990**, *11*, 440.
(22) Frisch, M. J.; Trucks, G. W.; Schlegel, H. B.; Scuseria, G. E.; Robb, M. A.; Cheeseman, J. R.; Zakrzewski, V. G.; Montgomery, J. A., Jr.; Stratmann, R. E.; Burant, J. C.; Dapprich, S.; Millam, J. M.; Daniels, A. D.; Kudin, K. N.; Strain, M. C.; Farkas, O.; Tomasi, J.; Barone, V.; Cossi, M.; Cammi, R.; Mennucci, B.; Pomelli, C.; Adamo, C.; Clifford, S.; Ochterski, J.; Petersson, G. A.; Ayala, P. Y.; Cui, Q.; Morokuma, K.; Malick, D. K.; Rabuck, A. D.; Raghavachari, K.; Foresman, J. B.; Cioslowski, J.; Ortiz, J. V.; Stefanov, B. B.; Liu, G.; Liashenko, A.; Piskorz, P.; Komaromi, I.; Gomperts, R.; Martin, R. L.; Fox, D. J.; Keith, T.; Al-Laham, M. A.; Peng, C. Y.; Nanayakkara, A.; Gonzalez, C.; Challacombe, M.; Gill, P. M. W.; Johnson, B. G.; Chen, W.; Wong, M. W.; Andres, J. L.; Head-Gordon, M.; Replogle, E. S.; Pople, J. A. *Gaussian 03*, revision A.9; Gaussian, Inc.: Pittsburgh, PA, 2003.
(23) This was confirmed in a few cases by performing the optimization in Cartesian space (no redundant internal coordinates) and using steepest descents. The energy monotonically decreased as the optimization proceeded and the proton transferred.
(24) See ref 4. The carboxylic acid proton in 2,5-DHB$^+$ has a gas-phase acidity that is lower than that of 3,5-DHB$^+$ by about 56 kJ/mol (thus, 2,5-DHB$^+$ is more acidic at the carboxylic site). This is due to the same phenomenon observed here in the clusters: Loss of the carboxylic acid proton in the 2,5-isomer results in a second intermolecular transfer from the 2-OH to the carboxylic acid group.
(25) Ueno-Noto, K.; Marynick, D. S. Manuscript in preparation.